Population Dynamics in a Changing Environment: Random versus Periodic Switching

Ami Taitelbaum[§],[1] Robert West[§],[2] Michael Assaf,[1,*] and Mauro Mobilia[2,†]

[1]*Racah Institute of Physics, Hebrew University of Jerusalem, Jerusalem 91904, Israel*
[2]*Department of Applied Mathematics, School of Mathematics, University of Leeds, Leeds LS2 9JT, U.K.*

Environmental changes greatly influence the evolution of populations. Here, we study the dynamics of a population of two strains, one growing slightly faster than the other, competing for resources in a time-varying binary environment modeled by a carrying capacity that switches either *randomly* or *periodically* between states of abundance and scarcity. The population dynamics is characterized by demographic noise (birth and death events) coupled to the fluctuating population size. By combining analytical and simulation methods, we elucidate the similarities and differences of evolving subject to stochastic and periodic switching. We show that the population size distribution is broader under intermediate and fast random switching than under periodic variations, with periodic changes leading to an abrupt transition from slow to fast switching regimes. The fixation probability under intermediate/fast random and periodic switching can hence vary significantly, with markedly different asymptotic behaviors. We also determine the conditions under which the fixation probability of the slow strain is optimal when the dynamics is driven by asymmetric switching.

PACS numbers:

The evolution of natural populations is influenced by varying environmental conditions. Here, the abundance of nutrients, toxins, or external factors like temperature are subject to random and seasonal variations, and have an important impact on population dynamics [1, 2].

Several mechanisms have been suggested for a population to cope with changing environments by assuming that external factors vary either periodically or stochastically in time [3–21]. A common choice to model external variations, both for its simplicity and experimental relevance, is to consider an environment that periodically or stochastically switches between two states [22–41]. In finite populations, demographic noise (DN) is another important form of randomness that can lead to fixation (one species takes over the population [42, 43]). DN tends to be strong in small populations and negligible in large ones. Importantly, the evolution of a population composition is often coupled with the dynamics of its size [44–49]. This can lead to DN being coupled to environmental variability (EV), with external factors affecting the population size, which in turn modulates the DN strength. The interplay between EV and DN is important in various fields, *e.g.*, in gene regulatory networks, see [13, 17] and references therein. In particular, it is relevant to microbial communities, which are often volatile and subject to extreme environmental changes [50–55]. These may lead to *population bottlenecks* where new colonies consisting of few individuals are prone to fluctuations.

In most studies, fluctuations stemming from EV and DN are considered to be independent, often by assuming that growth rates vary independently of the population [5, 6, 10–18, 20, 22–24, 26, 31–33, 36, 38]. In this context, there is as yet no systematic comparison of the evolution under random and periodic switching: some works report that they lead to similar evolutionary processes while others find differences, see *e.g.*, Refs. [24, 35]. Here, we systematically study the *coupled influence* of EV and DN on the evolution of a population where slow- and fast-growing strains compete for resources subject to a randomly and periodically switching carrying capacity.

A distinctive feature of this model is that it accounts for the stochastic or periodic depletion and recovery of resources via a binary environment that varies with a finite correlation time or period, see Fig. 1. This setting is motivated by realistic situations, but is simple enough to enable analytical progress. Indeed, while the cases of binary random and periodic switching are idealizations of real-world environments, they serve as baseline models to understand whether environmental perturbations of different nature lead to the same dynamics.

Using a combination of analytical and computational tools, we address the fundamental question of comparing the evolution subject to stochastic and deterministic changes by considering random versus periodic environmental switching. This is done by elucidating the influence of EV on the population size distribution (PSD) and its fixation properties. We analytically show that the PSD is broader under intermediate and fast random switching than under periodic switching, with the latter leading to a more abrupt transition from slow to fast switching regime. Consequently, the fixation probability under intermediate/fast random and periodic switching can vary significantly and exhibit markedly different asymptotic behaviors. We also determine the nontrivial asymmetric switching conditions under which the fixation probability of the slow strain is optimal.

We consider a well-mixed population of time-fluctuating size $N(t) = N_S(t) + N_F(t)$ consisting of two strains. At time t, $N_S(t)$ individuals are of a slow-

[§]The authors contributed equally to this work.

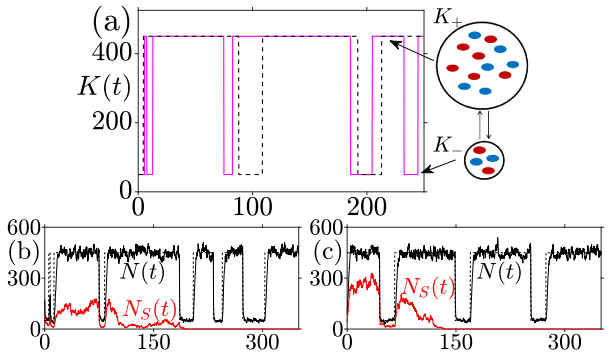

FIG. 1: (a) Asymmetric random (pink/light gray) and periodic (black dashed) switching between $K = K_+$ and $K = K_-$ with rates $\nu_\pm$ causes the fluctuation of the population size (large/small circles) whose composition changes until fixation occurs as in (b) and (c), see text. (b, c) Typical single realizations of N (black) and N_S (red/gray) vs. time under random (b) and periodic (c) switching. Parameters: $(s, K_0, \nu, \gamma, \delta, x_0) = (0.02, 250, 0.03, 0.8, 0.6, 0.5)$.

growing strain S, corresponding to a fraction $x = N_S/N$ of the population, and N_F are of a fast-growing species F. Individuals of strain S and F reproduce with respective per-capita growth rates $(1-s)/\bar{f}$ and $1/\bar{f}$, where $\bar{f} = (1-s)x + 1 - x = 1 - sx$ is the population's average fitness, and $0 < s \ll 1$ is the selection intensity denoting the small growth advantage of F over S [39, 40, 45, 46]. The strains's growth is limited by a logistic death rate N/K, where $K \gg 1$ is the carrying capacity. Population dynamics is often idealized by assuming a static environment (constant K) which yields a constant or logistically-varying population size [43, 56–59]. Here, we instead consider a fluctuating population size subject to a time-varying environment, which evolves according to the birth-death process [40, 62]:

$$N_{S/F} \xrightarrow{T^+_{S/F}} N_{S/F} + 1 \quad \text{and} \quad N_{S/F} \xrightarrow{T^-_{S/F}} N_{S/F} - 1, \quad (1)$$

with transition rates $T^+_S = (1-s)N_S/\bar{f}$, $T^+_F = N_F/\bar{f}$ and $T^-_{S/F} = (N/K)N_{S/F}$. We model EV via a switching carrying capacity

$$K(t) = K_0[1 + \gamma\xi_\alpha(t)], \quad \text{with} \quad \xi_\alpha(t) \in \{-1, +1\}, \quad (2)$$
$$K_0 \equiv \frac{K_+ + K_-}{2} \quad \text{and} \quad \gamma \equiv \frac{K_+ - K_-}{2K_0},$$

where $\alpha \in \{r, p\}$ and $\gamma = \mathcal{O}(1)$. Here, resources vary either randomly ($\alpha = r$) or periodically ($\alpha = p$), between states of scarcity, $K = K_-$ ($\xi_\alpha = -1$), and abundance, $K = K_+ > K_-$ ($\xi_\alpha = +1$), causing fluctuations of the population size and its composition, see Fig. 1.

When $K(t)$ switches *randomly*, ξ_r is a colored *asymmetric dichotomous (telegraph) Markov noise* (ADN) [60, 61], with the transition $\xi_r \to -\xi_r$ occurring at rate $\nu_\pm$ when $\xi_r = \pm 1$. It is useful to introduce the average switching rate $\nu = (\nu_+ + \nu_-)/2$ and $\delta = (\nu_- - \nu_+)/(2\nu)$, measuring the switching asymmetry ($|\delta| < 1$) [62]. Clearly, $\delta = 0$ denotes symmetric dichotomous noise [39, 40]. At stationarity, the ADN's mean and autocorrelation functions are $\langle\xi_r\rangle = \delta$ and $\langle\xi_r(t)\xi_r(t')\rangle - \langle\xi_r(t)\rangle\langle\xi_r(t')\rangle = (1-\delta^2)\, e^{-2\nu|t-t'|}$ (where $\langle\cdot\rangle$ denotes ensemble averaging). When $K(t)$ switches *periodically*, ξ_p is a *rectangular wave* defined in terms of the rectangular function, rec$(\cdot)$ [63], of period T:

$$\xi_p = \sum_{j=-\infty}^{\infty} \left\{ \text{rec}\left(\frac{t + \frac{1}{2\nu_+} + jT}{1/\nu_+} \right) - \text{rec}\left(\frac{t - \frac{1}{2\nu_-} + jT}{1/\nu_-} \right) \right\},$$

where $T = (1/\nu_+) + (1/\nu_-) = 2/[(1-\delta^2)\nu]$. When $\delta = 0$, this reduces to the square wave $\xi_p(t) = \text{sign}\{\sin(\pi\nu t)\}$. At stationarity, ξ_p averaged over one period has the same mean and correlation function as ξ_r. Henceforth we consider ξ_r and ξ_p at stationarity, and the mean and variance of $K(t)$ are thus the same for $\alpha \in \{r, p\}$ and given by $\langle K\rangle = K_0(1 + \gamma\delta)$ and $\text{var}(K) = (\gamma K_0)^2(1-\delta^2)$ [64], which increases with γ and decreases with $|\delta|$.

Upon ignoring the eventual extinction of the population which occurs after an enormous time (unobservable when $K_0 \gg 1$) [39] [**?**], the main features of this evolutionary model are the long-time *population size distribution* (PSD) and the species *fixation probability*. These quantities, describing the system's ecological and evolutionary dynamics, can be found by analyzing the underlying master equation [40, 41, 62, 66, 67].

Insight into the dynamics can be gained by ignoring fluctuations and considering the mean-field picture of a very large population subject to constant $K = K_0$. Here, the population size N and x evolve according to $\dot{N} \equiv (d/dt)N = N(1 - N/K_0)$ and $\dot{x} = -sx(1-x)/(1-sx)$ [45, 46, 62, 65], which predict that x decays on a timescale $t \sim 1/s \gg 1$, while $N(t) = \mathcal{O}(K_0)$ after $t = \mathcal{O}(1)$. Thus, a timescale separation occurs when $s \ll 1$: the typical relaxation time of x is much slower than that of N. Yet, a finite population is subject to DN (randomly occurring birth and death events), resulting in the eventual fixation of one of the species. Here, given a fixed population size N, the S fixation probability starting from an initial fraction $x_0 = N_S(0)/N(0)$ is [43, 58, 67]

$$\phi(x_0)|_N = \left[e^{-Nx_0\ln(1-s)} - 1\right] / \left[e^{-N\ln(1-s)} - 1\right], \quad (3)$$

which exponentially decreases with N. For $s \ll N^{-1/2} \ll 1$ ("diffusion approximation"), this result simplifies to $\phi(x_0)|_N \simeq (e^{-Ns(1-x_0)} - e^{-Ns})/(1 - e^{-Ns})$ [39, 40, 57]. Eq. (3) also gives the approximate fixation probability when N fluctuates about constant $K = K_0$.

This scenario significantly changes when in addition to DN, the population is subject to a time-varying carrying capacity, see Fig. 1. Inspired by the drastic changes in the environment of microbial communities at different frequencies [50–54], we study below the influence of the EV (ν, γ, and δ) on the PSD and fixation properties.

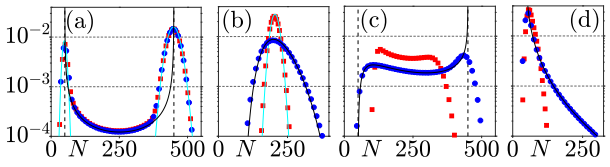

FIG. 2: $P_\nu^{(r)}(N)$ (blue/dark gray) and $P_\nu^{(p)}(N)$ (red/gray) for different ν: (a) $\nu = 0.05$, (b) $\nu = 17.5$, (c) $\nu = 1.4$, (d) $\nu = 1$. Symbols are from simulations; solid black lines in (a,b) are from (4), those in cyan/light gray are from $P_0(N)$ in (a) and (5) in (b); vertical dashed lines in (a,c) show $N = K_\pm$; horizontal dashed lines are eyeguides. Here $(s, K_0, \gamma, x_0) = (0.05, 250, 0.8, 0.5)$, $\delta = 0.7$ in (a)-(c) and $\delta = -0.5$ in (d).

Population size distribution. Simulations show that the marginal quasi-stationary PSD, $P_\nu^{(\alpha)}(N)$ (unconditioned of ξ_α), is characterized by different regimes depending on the switching rate ν, with markedly different features in the case of random and periodic switching when $\nu = \mathcal{O}(1)$ and $\nu \gg 1$, see Fig. 2.

The case of random switching can be treated similarly to $\delta = 0$ (symmetric dichotomous noise) [39, 40]. Here, we ignore DN and assume that the population size is driven only by ADN according to the piecewise-deterministic Markov process (PDMP) [62, 68, 69], defined by the stochastic differential equation $\dot{N} = N\,[1 - (N/\mathcal{K})(1 - \gamma\xi_r)/(1 - \gamma\delta)]$, where $\mathcal{K} \equiv K_0(1 - \gamma^2)/(1 - \gamma\delta)$. When $\nu \to \infty$, the ADN self-averages, $\xi \xrightarrow{\nu\to\infty} \langle\xi\rangle = \delta$, and $N \xrightarrow{\nu\to\infty} \mathcal{K}$. Therefore, the marginal PSD [40, 60] of this PDMP satisfies

$$P_\nu^{\rm PDMP}(N) \propto \frac{1}{N^2}\left(\frac{K_+}{N} - 1\right)^{\nu_+ - 1}\left(1 - \frac{K_-}{N}\right)^{\nu_- - 1}, \quad (4)$$

where the normalization constant has been omitted, and the dependence on γ, δ and ν is given by $K_\pm = (1 \pm \gamma)K_0$ and $\nu_\pm = (1 \mp \delta)\nu$. Although $P_\nu^{\rm PDMP}$ has support $[K_-, K_+]$ and only accounts for EV, when $K_0 \gg 1$ and $\gamma = \mathcal{O}(1)$, it captures the peaks of $P_\nu^{(r)}$ and the average population size, see Figs. 2 and S3(b) in [62], which are the most relevant features for the population fixation properties. Clearly, $P_\nu^{\rm PDMP}$ ignores DN and cannot capture the width of $P_\nu^{(r)}$ about its peaks, see Fig. 2 (a,c,d). Yet, this can be remedied by a linear noise approximation about the PDMP, see [40] and Sec. 3.2 in [62].

For periodic switching, $P_\nu^{(p)}$ can be found analytically in the limits of very slow ($\nu \to 0$) and fast ($\nu \gg 1$) switching. For $\nu \to 0$ the carrying capacity is initially randomly allocated and is almost constant, i.e. $K(t) \simeq K(0)$. The PSD is thus the same in the periodic and random switching: $P_0^{(p)} = P_0^{(r)} \equiv P_0$, and can be computed from the master equation. Assuming $K_0 \gg 1$ and $\gamma = \mathcal{O}(1)$, the PSD turns out to be bimodal with peaks about $N = K_\pm$, whose intensity depends on δ [62]: $P_0(N) \simeq [(1+\delta)\,K_+^{N+1}e^{-K_+} + (1-\delta)\,K_-^{N+1}e^{-K_-}]/[2(N+1)!]$. This result excellently agrees with simulations, see Fig. 2 (a).

Under fast periodic switching, $P_\nu^{(p)}$ differs markedly from its random counterpart, see Fig. 2 (b). An approximate expression of $P_\nu^{(p)}$ to leading order in $1/\nu$ can be obtained from the master equation using the WKB approximation [70] and Kapitza method [11, 20, 71]. The latter involves separating the dynamics into fast and slow variables, and averaging the fast variables. As shown in Sec. 2.2 of [62], this yields (up to a normalization factor)

$$P_\nu^{\rm Kap} \sim \mathcal{P}(N)\,\exp\left[-\frac{K_0}{72\nu^2}\left(\frac{\gamma}{1-\gamma^2}\right)^2\left(\frac{2N-\mathcal{K}}{K_0}\right)^3\right], \quad (5)$$

where $\mathcal{P}(N) \propto \exp[N(1 - \ln(N/\mathcal{K}))]$ is the PSD at $\nu \to \infty$, peaked at $N = \mathcal{K}$. We notice that both $P_\nu^{(p)} \simeq P_\nu^{\rm Kap}$ and $P_\nu^{(r)} \simeq P_\nu^{\rm PDMP}$ are unimodal and peaked at $N \approx \mathcal{K}$ when $\nu \gg 1$, but $P_\nu^{\rm Kap}$ is significantly sharper and narrower than $P_\nu^{\rm PDMP}$. In fact, the variance of $P_\nu^{\rm PDMP}$ scales as K_0^2/ν when $1 \ll \nu \ll K_0$, and is much larger than the variance of $P_\nu^{\rm Kap}$ which is of order K_0, see Sec. 4.3 in [62].

Note that while P_0 and $P_\nu^{\rm Kap}$ [Eq. (5)] account for DN *and* EV, $P_\nu^{\rm PDMP}$ [Eq. (4)] only accounts for EV. Yet, in the regime $1 \lesssim \nu \ll K_0$, DN is negligible compared to EV [62], and $P_\nu^{\rm PDMP}$ provides a suitable description of $P_\nu^{(r)}$ in this regime. In particular, $P_\nu^{\rm PDMP}$ allows us to characterize interesting phenomena arising in the intermediate *asymmetric* switching regime where $\nu \gtrsim 1$ with $\nu_- > 1$ and $\nu_+ < 1$ (longer sojourn in state $K = K_+$), or $\nu_- < 1$ and $\nu_+ > 1$, i.e. when $1/(1+|\delta|) < \nu < 1/(1-|\delta|)$. In the former case ($\delta > 0$), $P_\nu^{(r)}$ has a peak at $N \approx K_+$ and, under sufficiently strong EV, exhibits also a peak N^* between K_- and K_+ (i.e. $K_- < N^* < K_+$), whose position is aptly captured by Eq. (4), see Fig. 2(c) and Sec. 3.1 in [62]. In Fig. 2(c), one can see that $P_\nu^{(p)}$ also has two peaks, but it is narrower than $P_\nu^{(r)}$. When $\nu \gtrsim 1$, with $\nu_- < 1$ and $\nu_+ > 1$ ($\delta < 0$), $P_\nu^{(r)}$ exhibits a single peak at $N \approx K_-$, again well predicted by Eq. (4), see Fig. 2(d). Here, $P_\nu^{(p)}$ exhibits this same peak, but is again narrower than $P_\nu^{(r)}$. In fact, Fig. 2 shows that the transition from bimodal to unimodal PSD (slow to fast switching) is more abrupt under periodic than under random switching. This results in a dramatic change in the fixation probability's asymptotic behavior, see below.

Fixation probability. When $s \ll 1$, at $t \gtrsim \mathcal{O}(1)$, once the system has settled in its long-lived PSD, given an initial fraction x_0 of S individuals, the S-species fixation probability subject to α-switching ($\alpha \in \{r, p\}$), ϕ_α, can be approximated by averaging $\phi(x_0)|_N$ over $P_{\nu/s}^{(\alpha)}(N)$, upon rescaling $\nu \to \nu/s$ [39, 40]:

$$\phi_\alpha(\nu) \simeq \int_0^\infty P_{\nu/s}^{(\alpha)}(N)\;\phi(x_0)|_N\;dN, \quad \alpha \in \{r, p\}. \quad (6)$$

This result is valid under weak selection, $1/K_0 \ll s \ll 1$, when there are $\mathcal{O}(\nu/s)$ switches prior to fixation [39, 40,

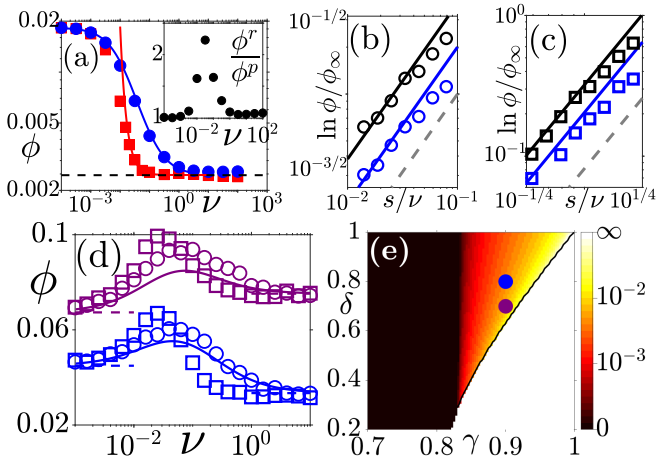

FIG. 3: (a)-(d) fixation probability for random/periodic switching (circles/squares): symbols are from simulations. In (a) solid lines are from Eqs. (7) and (S33) of [62] for periodic and random switching, respectively. In (b,c), solid lines are from (7) and, in (d), from (S33) of [62]. Here $(s, K_0, \gamma, x_0) = (0.025, 800, 0.7, 0.5)$ in (a)-(c) and $(s, K_0, \gamma, x_0) = (0.05, 250, 0.9, 0.6)$ in (d,e). (a) ϕ_α versus ν with $\delta = 0.2$; dashed line shows $\phi^{(\infty)}$. Inset: ϕ_r/ϕ_p versus ν with $\delta = 0.2$. (b,c) $\ln(\phi_\alpha/\phi^{(\infty)})$ versus s/ν for random (b) and periodic (c) switching with $\delta = 0.2$ (black) and $\delta = 0$ (blue/dark gray). Dashed gray lines are eyeguides $\propto s/\nu$ in (b) and $\propto (s/\nu)^2$ in (c). (d) Non-monotonic $\phi_\alpha(\nu)$ with $\delta = 0.7$ (purple/dark gray) and $\delta = 0.8$ (blue/black); dashed lines show $\phi^{(0,\infty)}$. $\phi_r(\nu)$ and $\phi_p(\nu)$ are maximal at $\nu = \nu_r^* \approx 0.1$ and $\nu = \nu_p^* \approx 0.07$, see text. (e) Heatmap of ν_r^* (see Sec. 5.1 in [62] for details): $\nu_r^* \to 0, \infty$ in the black and white areas, respectively; $\phi_r(\nu)$ is non-monotonic in the red-yellow/gray area, with $\nu_r^* \approx 0.01$ (red/dark gray) - $\nu_r^* \approx 0.1$ (yellow/light gray), see vertical bar. Symbols are for $\gamma = 0.9$, $\delta = 0.7$ (purple/dark gray) and $\delta = 0.8$ (blue/black).

62]. The difference between ϕ_r and ϕ_p stems from the different ν-dependence of $P_\nu^{(r)}$ and $P_\nu^{(p)}$, see Figs. 2 . In the case of random switching $\phi_r(\nu)$ can be approximated by substituting Eq. (4) into (6), yielding Eq. (S33) of [62], which is valid over a broad range of ν [39, 62], as confirmed by simulations, see Fig. 3 and S2(c,d) of [62].

When $\nu \to 0$ (slow switching), there are no switches prior to fixation and the population density is peaked at $N = K_\pm$ under random and periodic switching. Hence, with (6), we approximate $\lim_{\nu\to 0}\phi_\alpha(\nu) \simeq \phi^{(0)} = [(1-\delta)\phi(x_0)|_{K_-} + (1+\delta)\phi(x_0)|_{K_+}]/2$. In Fig. 3(d) we confirm that, when $\nu/s \ll 1$, $\phi^{(0)}$ coincides with $\phi_r(\nu)$ and $\phi_p(\nu)$.

When $\nu/s \gg 1$ (fast switching), $P_{\nu/s}^{(\alpha)}$ is sharply peaked at $N \simeq \mathcal{K}$, see Fig. 2(b), and to leading order $\lim_{\nu\to\infty}\phi_\alpha(\nu) \simeq \phi^{(\infty)} = \phi(x_0)|_{\mathcal{K}}$ [39, 40]. Simulation results of Fig. 3 confirm that at $\nu \gg s$, $\phi_r(\nu)$ and $\phi_p(\nu)$ converge to $\phi^{(\infty)}$. Thus, the fixation probability under fast random/periodic switching is the same to lowest order in $1/\nu$. Yet, the rate of convergence to $\phi^{(\infty)}$ is different in the random and periodic case, see Fig. 3(a). This is explained by computing the next-to-leading order of ϕ_α in $\nu/s \gg 1$. For this, along with (3), we use Eq. (S33) of [62] for random switching and substitute (5) into (6) for periodic switching. A saddle-point calculation, with $1/K_0 \ll s \ll 1$, yields (see Sec. 4 in [62])

$$\ln\left(\frac{\phi_\alpha(\nu)}{\phi^{(\infty)}}\right) \simeq \begin{cases} \mathcal{A}_r(s/\nu) & (\alpha = r) \\ \mathcal{A}_p\ (s/\nu)^2 & (\alpha = p). \end{cases} \tag{7}$$

Here $\phi^{(\infty)} = e^{m/2}$, $m \equiv 2\mathcal{K}(1-x_0)\ln(1-s)$, and $\mathcal{A}_r = m(4+m)(1-\delta^2)(\gamma/(1-\gamma\delta))^2/16$ while $\mathcal{A}_p = \mathcal{K}(1-(1+m/\mathcal{K})^3)(\gamma/(1-\gamma\delta))^2/72$. Thus, when $K_0 s \gg 1$, $\phi_\alpha(\nu)$ converges to $\phi^{(\infty)}$ much faster for $\alpha = p$ than when $\alpha = r$, see Fig. 3(a)-(c); i.e., the fixation probability exhibits markedly different behaviors under periodic and random switching. Also, the ratio ϕ_r/ϕ_p [see inset of Fig. 3(a)] has a sharp peak at a nontrivial intermediate ν.

Under intermediate switching, ϕ_α exhibits a rich behaviour as ν increases and ϕ_α interpolates between $\phi^{(0)}$ and $\phi^{(\infty)}$, see Fig. 3(d). Under large enough switching asymmetry, ϕ_α is a non-monotonic function of ν in a nontrivial region $\gamma > \gamma_c(s)$, $\delta > \delta_c(\gamma, s)$ of the parameter space that can be found from (6), see Fig. 3 (d,e) and Sec. 5.1 in [62]. The PDMP-based approximation [Eq. (S33) in [62]] captures reasonably well the ν-dependence of ϕ_r in this regime, and that it has a clear maximum at $\nu_r^* \sim s$. This optimal switching rate for the S species fixation at given γ, δ and s corresponds to $\mathcal{O}(1)$ switches prior to fixation, while $\phi_r(\nu_r^*)/\max(\phi^{(0)}, \phi^{(\infty)}) - 1$ reaches up to 30%, see Fig. 3 (d,e). Similar results are found for periodic switching with an optimal switching rate $\nu_p^* \lesssim \nu_r^*$ and a sharper/narrower peak $\phi_p(\nu_p^*)$. The existence of a maximum $\phi_\alpha(\nu_\alpha^*)$ is thus a signature of asymmetric switching. For intermediate switching rate and not too large asymmetry ($|\delta| < \delta_c$), $\phi_r(\nu)$ is a monotonic function: it increases/decreases with ν above/below a critical selection intensity s_c (with γ, δ fixed), that we have determined, see Fig. S2(b) and Sec. 5.2 in [62]. A similar qualitative behavior is observed for $\phi_p(\nu)$.

Remarkably, similar qualitative results are obtained in the more intricate case of eco-evolutionary dynamics, arising when the slow strain produces public goods benefiting the entire population, see Sec. 7 and Fig. S4 in [62].

Inspired by the evolution of microbial communities in fluctuating environments, we have studied the dynamics of a population of two strains, one growing slightly faster than the other, competing for resources in a binary environment. Importantly, our model accounts for coupling between demographic noise and environmental variability, where the latter has been modeled by a carrying capacity that switches between states of scarcity/abundance *randomly* or *periodically* in time. Here, we have systematically compared the effects of random and periodic switching on the population size and its fixation properties. Our findings hence highlight the effect of evolving subject to a stochastically- versus

deterministically-varying environment. We have shown that the population size distribution is broader under intermediate and fast random switching than under periodic change, with a more abrupt transition from the slow to fast switching regime in the periodic case. As a consequence we have found markedly different asymptotic behaviors of the fixation probability under fast random and periodic switching. We have also determined the nontrivial asymmetric switching conditions of the environment under which the probability that the slow species prevails is optimal. Our work elucidates the similarities and differences of evolution under randomly/periodically-varying environments. These are particularly relevant to microbial communities, subject to frequent environmental changes.

We are grateful to E. Frey, A. M. Rucklidge, and K. Wienand for useful discussions. The support of an EPSRC Ph.D. studentship to RW (Grant No. EP/N509681/1) is gratefully acknowledged. AT and MA also acknowledge support from the Israel Science Foundation grant No. 300/14 and the United States-Israel Binational Science Foundation grant No. 2016-655.

* Electronic address: michael.assaf@mail.huji.ac.il
† Electronic address: M.Mobilia@leeds.ac.uk

[1] C. R. Morley, J. A. Trofymow, D. C. Coleman, and C. Cambardella, Microbiol. Ecol. **9**, 329 (1983).
[2] C. A. Fux, J. W. Costerton, P. S. Stewart, and P. Stoodley, Trends Microbiol. **13**, 34 (2005).
[3] H. Beaumont, J. Gallie, C. Kost, G. Ferguson, and P. Rainey, Nature **462**, 90 (2009).
[4] P. Visco, R. J. Allen, S. N. Majumdar, and M. R. Evans, Biophys. J. **98**, 1099 (2010).
[5] R. M. May, *Stability and complexity in model ecosystems* (Princeton University Press, Princeton, USA, 1973).
[6] S. Karlin and B. Levikson, T. Pop. Biol. **6**, 383 (1974).
[7] P. L. Chesson and R. R. Warner, American Naturalist **117**, 923 (1981).
[8] M. Loreau and C. de Mazancourt, American Naturalist **172**, E49 (2008).
[9] B. K. Xue and S. Leibler, Phys. Rev. Lett. **119**, 108103 (2017).
[10] E. Kussell and S. Leibler, Science **309**, 2075 (2005).
[11] M. Assaf, A. Kamenev and B. Meerson, Phys. Rev. E. 78, 041123 (2008).
[12] M. Assaf, A. Kamenev and B. Meerson, Phys. Rev. E. 79, 011127 (2009).
[13] M. Assaf, E. Roberts, Z. Luthey-Schulten, and N. Goldenfeld, Phys. Rev. Lett. **111**, 058102 (2013).
[14] Q. He, M.Mobilia, and U. C. Täuber, Phys. Rev. E **82**, 051909 (2010).
[15] U. Dobramysl, and U. C. Täuber, Phys. Rev. Lett. **110**, 048105 (2013).
[16] M. Assaf, M. Mobilia, and E. Roberts, Phys. Rev. Lett. **111**, 238101 (2013).
[17] E. Roberts, S. Be'er, C. Bohrer, R. Sharma and M. Assaf, Phys. Rev. E. 92, 062717 (2015).
[18] A. Melbinger and M. Vergassola, Scientific Reports **5**, 15211 (2015).
[19] M. Assaf and B. Meerson, J. Phys. A: Math and Theo. 50, 263001 (2017).
[20] O. Vilk and M. Assaf, Phys. Rev. E. 97, 062114 (2018).
[21] U. Dobramysl, M. Mobilia, M. Pleimling, and U. C. Täuber, J. Phys. A: Math. Theor. **51**, 063001 (2018).
[22] E. Kussell, R. Kishony, N. Q. Balaban, and S. Leibler, Genetics **169**, 1807 (2005).
[23] M. Acar, J. Mettetal, and A. van Oudenaarden, Nature Genetics **40**, 471 (2008).
[24] M. Thattai and A. Van Oudenaarden, Genetics **167**, 523 (2004).
[25] S. P. Otto and M. C. Whitlock, Genetics **146**, 723 (1997).
[26] B. Gaál, J. W. Pitchford, and A. J. Wood, Genetics **184**, 1113 (2010).
[27] K. Wienand, MSc Thesis (Ludwig-Maximilians-Universität München, 2011).
[28] P. Patra and S. Klumpp, PLoS ONE **8**(5): e62814 (2013).
[29] P. Patra and S. Klumpp, Phys. Biol. **12** 046004 (2015).
[30] E. A. Yurtsev, H. X. Chao, M. S. Datta, T. Artemova and J. Gore, Molecular Systems Biology **9**, 683 (2013).
[31] P. Ashcroft, P. M. Altrock, and T. Galla, J. R. Soc. Interface **11**, 20140663 (2014).
[32] M. Danino M and N. M. Shnerb, J. Theor. Biol. **441**, 84 (2018).
[33] P. G. Hufton, Y. T. Lin, and T. Galla, J. Stat. Mech. Theory Exp. **023501** (2018).
[34] Q. Su, A. McAvoy, L. Wang, and M. A. Nowak, Proc. Natl. Acad. Sci. USA **116**, 25398 (2019).
[35] I. Meyer and N. M. Shnerb, e-print: arXiv1912.06386.
[36] P. G. Hufton, Y. T. Lin, T. Galla, and A. J. McKane, Phys. Rev. E **93**, 052119 (2016).
[37] J. Hidalgo, S. Suweis, and A. Maritan, J. Theor. Biol. **413**, 1 (2017).
[38] R. West, M. Mobilia, and A. M. Rucklidge, Phys. Rev. E **97**, 022406 (2018).
[39] K. Wienand, E. Frey, and M. Mobilia, Phys. Rev. Lett **119**, 158301 (2017).
[40] K. Wienand, E. Frey, and M. Mobilia, J. R. Soc. Interface **15**, 20180343 (2018).
[41] R. West and M. Mobilia, J. Theor. Biol. **491**, 110135 (2020).
[42] J. F. Crow and M. Kimura, *An Introduction to Population Genetics Theory* (Blackburn Press, New Jersey, 2009).
[43] W. J. Ewens, *Mathematical Population Genetics* (Springer, New York, 2004).
[44] J. Roughgarden, *Theory of Population Genetics and Evolutionary Ecology: An Introduction* (Macmillan, New York, 1979).
[45] A. Melbinger, J. Cremer, and E. Frey, Phys. Rev. Lett. **105**, 178101 (2010).
[46] J. Cremer, A. Melbinger, and E. Frey, Phys. Rev. E **84**, 051921 (2011).
[47] A. Melbinger, J. Cremer, and E. Frey, J. R. Soc. Interface **12**, 20150171 (2015).
[48] C. S. Gokhale and C. Hauert, Th. Pop. Biol. **111**, 28 (2016).
[49] J. S. Chuang, O. Rivoire, and S. Leibler, Science **323**, 272 (2009).
[50] L. M. Wahl, P. J. Gerrish, and I. Saika-Voivod, Genetics **162**, 961 (2002).
[51] K. Wienand, M. Lechner, F. Becker, H. Jung, and E.

Frey, PloS one, 10(8), e0134300 (2015).
[52] Z. Patwas and L. M. Wahl, Evolution **64**, 1166 (2009).
[53] M. A. Brockhurst, A. Buckling, and A. Gardner, Curr. Biol. **17**, 761 (2007).
[54] M. A. Brockhurst, PLoS One **2**, e634 (2007).
[55] J. Cremer, A. Melbinger, K. Wienand, T. Henriquez, H. Jung, and E. Frey, e-print: arXiv:1909.11338.
[56] P. A. P. Moran, *The statistical processes of evolutionary theory* (Clarendon, Oxford, 1962).
[57] R. A. Blythe and A. J. McKane, J. Stat. Mech. **P07018** (2007).
[58] T. Antal and I. Scheuring, Bull. Math. Biol. **68**, 1923 (2006).
[59] R. M. Nowak, *Evolutionary Dynamics* (Belknap Press, Cambridge, USA, 2006).
[60] W. Horsthemke and R. Lefever, *Noise-Induced Transitions* (Springer, Berlin, 2006).
[61] I. Bena, Int. J. Mod. Phys. B **20**, 2825 (2006).
[62] See Supplemental Material at http://link.aps.org/supplemental/10.1103/PhysRevLett.000.000000 for information about the simulations, the approximations of the PSD and (7), further details about Fig. 3, the mean fixation time results, and the generalization to a public good scenario.
[63] A rectangular function is defined as follows: $\mathrm{rec}(x) = 1$ if $|x| < 1/2$, $\mathrm{rec}(x) = 0$ if $|x| > 1/2$, while $\mathrm{rec}(\pm 1/2) = 0$.
[64] Here, $\langle\cdot\rangle$ is the ensemble average in the case of random switching ($\alpha = r$), and the average obtained by integrating over one period T, i.e. $\langle K(t)\rangle = (1/T)\int_t^{t+T} K(\tau)d\tau$, in the case of periodic switching ($\alpha = p$).
[65] When N and x are not coupled and $s \ll 1$, the initial condition $N(0)$ is irrelevant for our analysis. In our simulations we have considered either $N(0) = K_0$ or $N(0) = K_0(1-\gamma^2)/(1-\gamma\delta) = \mathcal{K}$, and have confirmed that our results are independent of the choice of $N(0)$.
[66] M. Assaf and B. Meerson, Phys. Rev. E. 81, 021116 (2010).
[67] S. Redner, *A Guide to First-Passage Processes*, (Cambridge, New York, 2001).
[68] K. Kitahara, W. Horsthemke, and R. Lefever, Phys. Lett. **70A**, 377 (1979).
[69] M. H. A. Davis, J. R. Stat. Soc. B **46**, 353 (1984).
[70] V. Elgart and A. Kamenev, Phys. Rev. E 70, 041106 (2004).
[71] L. D. Landau and E. M. Lifshitz, *Mechanics* (Pergamon, Oxford, 1976).
[72] After one species undergoes extinction, the other species has a logistic-like dynamics, see below. In this case, its mean time to extinction scales exponentially with its carrying capacity, see *e.g.* [19, 66].